Supplemental Document

optica

Surpassing soliton compression limits in anomalous dispersion high-power erbium fiber comb: supplement

KEVIN F. LEE,[1,*] GENGJI ZHOU,[2,3] YU YUN,[1] JIE JIANG,[1] HERBERT G. WINFUL,[4] AND MARTIN E. FERMANN[1]

[1] *IMRA America, Inc., 1044 Woodridge Avenue, Ann Arbor, Michigan 48105, USA*
[2] *Department of Physics, University of Michigan, 450 Church Street, Ann Arbor, Michigan 48109, USA*
[3] *State Key Laboratory of High Field Laser Physics, Shanghai Institute of Optics and Fine Mechanics, Chinese Academy of Sciences, Shanghai 201800, China*
[4] *Department of Electrical Engineering and Computer Science, University of Michigan, 1301 Beal Avenue, Ann Arbor, Michigan 48109, USA*
[*] *Corresponding author: klee@imra.com*

Supplement DOI: https://doi.org/10.6084/m9.figshare.14575341

Parent Article DOI: https://doi.org/10.1364/OPTICA.427977

Surpassing soliton compression limits in anomalous dispersion high power erbium fiber comb: supplemental document

This supplement compares different pulse shapes and the benefits of pulse shaping, presents scaling laws for application to different systems, and includes more details of the system and comb measurements.

1. NUMERICAL PULSE SHAPE OPTIMIZATION

Here we numerically investigate nonlinear fiber pulse compression in anomalous dispersion fiber with a variety of different pulse inputs, and how they evolve with pulse shaping optimization. We use full amplitude and phase, as well as phase only spectral domain pulse shaping. We find that Jacobi pulses are a good approximation to optimized pulse forms that allow for nonlinear pulse compression without reducing pulse quality as characterized by the Strehl ratio.

As in the Simulation section, the following is based on the standard nonlinear Schrödinger equation (Eqn. 1), with the chirped FBG compressor represented by an infinitesimally thin, strictly linear phase element, which produces the most salient features. The parameters here are based on the experimental values with an input pulse having 100 nJ energy, 250 fs FWHM, a chirped mirror pair with dispersion of -3700 fs^2 and a standard telecom fiber as a nonlinear compression element with a 4 cm length. The pulses are originally formed in the temporal domain, so the parabolic pulse will start with an unrealistically large bandwidth beyond the Er gain profile. We then use a stochastic parallel gradient descent algorithm [1] to optimize the fitness parameter $F = (peak\ power) \times (Strehl\ ratio)$ at the output of the system using spectral amplitude and phase changes at 30 spectral sampling points in a bandwidth of 30 THz (angular frequency). This bandwidth matches the actual pulse shaper, while the spectral resolution is around 4 times higher to reduce ringing in the time and spectral domains.

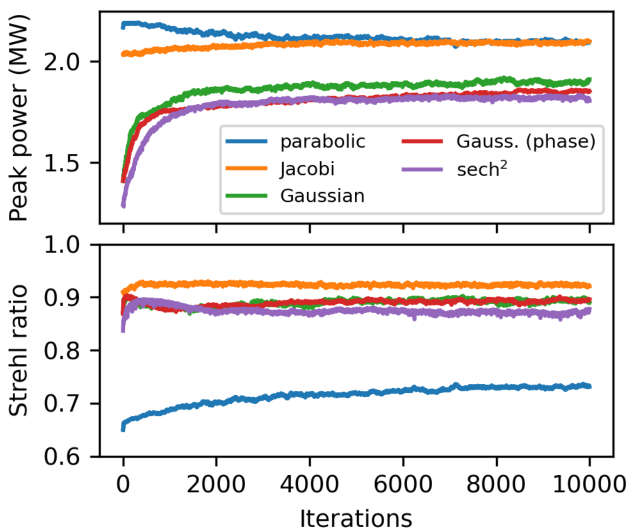

Fig. S1. Numerical optimization of output peak power and pulse quality as temporal Strehl ratio by phase and amplitude shaping of the input pulse. Labels indicate the initial pulse shape, (phase) indicates phase-only shaping.

Fig. S1 shows the progression of output peak power and the temporal Strehl ratio for pulse quality as the algorithm optimizes the phase and amplitude of the input pulse for different initial pulse shapes: an unchirped parabolic pulse, an unchirped Jacobi pulse, and chirped Gaussian and sech^2 pulses. For the Gaussian pulse input, we also show fitness improvement when using phase only pulse shaping with parameters matching the experimental shaper. Unlike the calculation in the main text, here all pulses have the same energy, which is why the parabolic and Jacobi pulses have higher peak power, as they have no tails.

Before optimization, the pulses rank as expected. The parabolic ideal has the highest peak power, but a poor Strehl ratio from the unrealistically broad spectrum. The Jacobi form has both high peak power, and good Strehl ratio from the reasonable bandwidth. Optimization does not cause much improvement of this already optimized form. The standard Gaussian and sech^2 pulses perform relatively poorly, but can be improved greatly by shaping into a Jacobi form. As the algorithm settles into a local minimum, the shaped standard pulses still have some wings around the peak, keeping the peak power lower than a pure Jacobi.

For the Gaussian, including amplitude shaping on top of phase shaping does not significantly improve the output, showing that a Gaussian spectrum is, at least locally, a good form. Using phase shaping increases the peak power here by about 30%, relative to a perfect Gaussian that has not been deformed in an amplifier, even with the relatively low resolution of the heated stretcher grating. A true Jacobi or nearly parabolic pulse could theoretically provide another 10 or 20%, but requires impractical broadening and shaping of the amplified spectrum.

Another way to look at the optimization starting from the Jacobi pulse is with the difference between the input Jacobi pulse and the shaped pulse given by the misfit parameter M:

$$M^2 = \frac{\int_{t_1}^{t_2} [P(t) - P_J(t)]^2 dt}{\int_{t_1}^{t_2} [P_J(t)]^2 dt} \tag{S1}$$

where P(t) is the power as a function of time of the shaped pulse, $P_J(t)$ is the power of the initial Jacobi pulse, and t_1 and t_2 are the truncation points where the initial Jacobi pulse goes to zero.

The misfit parameter as a function of iteration number is shown in Fig. S2. It stays below 0.012, showing that the small fitness improvement, even with high resolution amplitude and phase optimization, is not from a large change in the pulse shape. The spectral and phase differences with the optimized Gaussian are not very important, as the SPM in the propagation dominates. The algorithm is unable to significantly improve the Jacobi pulse, indicating it is a robust local maximum.

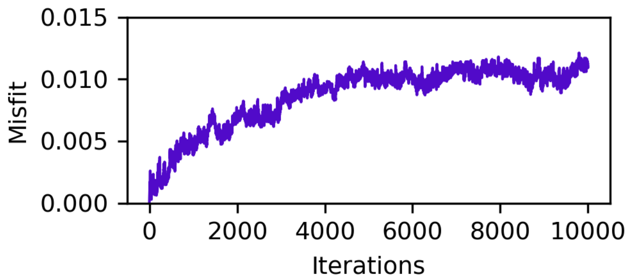

Fig. S2. Evolution of misfit parameter of a Jacobi pulse with iteration number while optimizing the fitness of the output pulse by phase and amplitude variation. The misfit parameter stays below 0.012.

2. SCALING

We consider here the propagation after a thin FBG compressor of an intense, unstretched input pulse through a short fiber, followed by chirped mirrors, and explore parameter scaling for different systems with similar performance characteristics. Spectral modification by self-phase modulation $\delta\omega$ is proportional to dI/dt (like plotted in Fig. 8 in the main text), fiber length z_{nl}, and the nonlinear parameter γ, so we can approximate $\delta\omega \propto \gamma z_{nl} P_0/\tau$ with peak power P_0, and temporal FWHM τ. The resulting chirp on the pulse is the frequency change with time proportional to $d^2 I/dt^2$, or approximately: $\delta\omega/\tau \propto \gamma z_{nl} P_0/\tau^2$.

We can use the first relation to maintain spectral broadening for different pulses by adjusting the fiber length according to $z_{nl} \approx C_1 \tau / \gamma P_0$, where $C_1 = 35\ \text{fs}^2$. The second relation tells us what chirped mirror dispersion D_2 is appropriate with $D_2 \approx C_2 \tau^2 / \gamma z_{nl} P_0$, with $C_2 = 0.25\ \text{m/s}^2$. The values for C_1 and C_2 are from our system parameters, and provide a guide for achieving similar behavior to our laser from different systems. We numerically verified these approximate scalings. The effective nonlinearity parameter γ is reduced by up to 100 times in large mode area fibers, meaning Jacobi pulse compression can be used at up to 40× higher energies, limited only by the self-focusing damage threshold of around 10 MW at 1.5 µm.

Beyond unstretched pulses, it is interesting to consider the potential for energy scaling with moderately chirped pulses and to what extent the Jacobi shape remains useful. In Figs. S3, we show optimal input pulse forms and their corresponding compressed shapes for input pulse energies of 100, 200, 400 and 800 nJ, while scaling the dispersion of the chirped mirrors by factors of 1, 2, 4 and 8. Here we use phase only pulse shaping to optimize the pulse form.

The Strehl ratio remains over 90% for all four pulse energies, and the pulses compress to less than 60 fs for 100, 200, and 400 nJ, and 75 fs for 800 nJ. The lower energy optimized pulses with less initial chirp are close to Jacobi shaped, while the two higher energy pulses with more chirp can more closely approach the ideal parabolic form, as in the main text discussion of the Jacobi pulse. If we were to further increase the initial chirp, spectral broadening would decrease, and the system would become more like a standard chirped pulse amplifier. If instead we maintain broadening and use large mode area fibers and pulse width scaling, a compact laser architecture producing µJ pulse energies at sub 100 fs pulses can be envisaged. With further compression in hollow core fibers [2], it will be possible to generate sub 10 fs pulses with high pulse quality in a compact form factor.

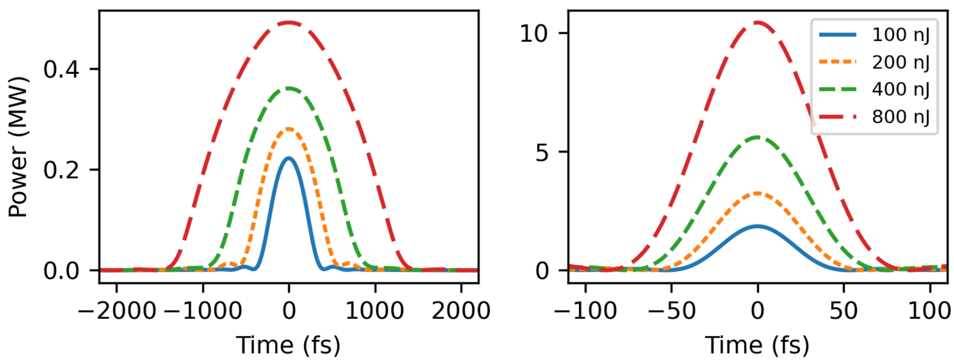

Fig. S3. Left: optimized injected pulse shape for nonlinear compression in 4 cm of fiber for 100, 200, 400 and 800 nJ. Right: compressed pulse forms after nonlinear propagation through 4 cm of fiber and linear pulse compression with a dispersive element. The dispersion of the chirped mirrors is increased proportionally to the pulse energy.

3. EXPERIMENTAL DETAILS

The laser system is illustrated in Fig. S4. The femtosecond comb oscillator (IMRA America, Inc. Ecomb 100T) outputs a spectrum centred around 1565 nm with FWHM of 54 nm. The stretched seed is first preamplified in backwards, core pumped Er fiber (iXBlue, 5 µm mode-field diameter) by 1 W at 976 nm. The main amplifier (Fibercore, 11 µm mode-field diameter) is backwards, cladding pumped by up to 36 W at 976 nm. The 100 MHz comb oscillator includes an additional core-pumped preamp. Most of the system is polarization maintaining (PM) except for the non-PM power amplifier and the filter and pump combiner attached to it.

Unlike a standard femtosecond fiber laser, the flexibility from pulse shaping means the particular fiber types and lengths are not very important here. The main requirements are: enough bandwidth to fill the stretcher and make use of the power amplifier gain bandwidth; the power amplifier core should not be small to avoid strong nonlinearity; and the pulse out of the fiber should be roughly compressed at low power.

The stretcher and compressor FBGs are the same design used in opposite directions (Teraxion), reflecting from 1540 to 1580 nm with dispersion of 10 ps/nm. The stretcher reflects the long wavelength side first. We estimate a stretched pulse duration of about 140 ps. The chirped mirrors (Ultrafast Innovations) have group delay dispersion of -460 fs^2, and third order dispersion of -2800 fs^3 per bounce, which is similar to linear transmission through 2 cm of PM1550 fiber. We used 8 bounces total, and the specified reflection is >99.9%. The actual total transmission was 97% including beam clipping.

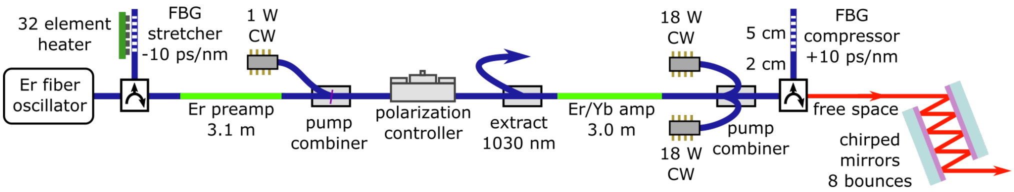

Fig. S4. Schematic of the laser system.

A. Spectral phase

Spectral phases for the short pulses at the three pulses energies discussed in the text are plotted in Fig. S5. Offset and linear slopes were manually subtracted. These adjustments were not propagated back into the temporal reconstructions plotted in the main text, which retain the automatic corrections of the commercial software. As expected for an SPM dominated process, the spectral wings have relatively clean phase, with significant structure in the centre where different spectral contributions interfere.

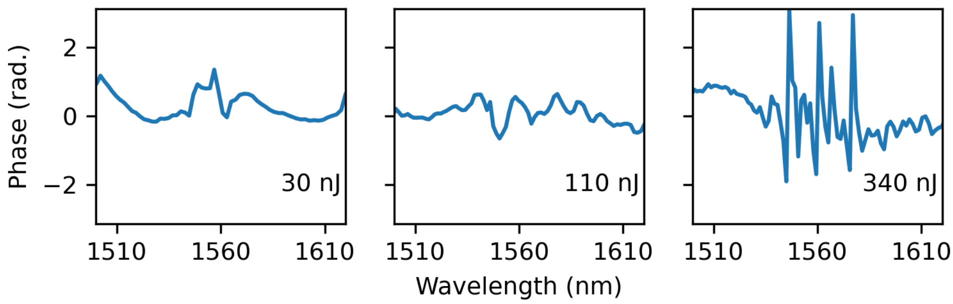

Fig. S5. Wrapped spectral phases of short pulses at the three pulse energies. The phase sign may be inverted from SHG FROG ambiguity. The spectral wings have similar phase, while the centre region is less clean.

B. Frequency comb

For the carrier envelope offset (CEO) frequency measurement, a small sample of the amplified 100 MHz free space beam was coupled back into a standard fiber f-2f interferometer. The spectrum was broadened in highly nonlinear fiber, the 2200 nm component was frequency doubled in periodically poled lithium niobate to 1100 nm, and the two 1100 nm beams interfere to generate the f-2f beat note. This beat note can then be stabilized by feedback to the CEO actuators of the oscillator.

An example of such a locked beat is plotted in orange on the left panel of Fig. S6, referenced to the peak of the carrier frequency. This is a measure of the lock quality, the less power out of the carrier, the better the lock. This is often converted to an integrated phase noise, shown in blue, with a value of about 0.3 rad integrated from 3 MHz to 1 Hz, indicating good lock quality.

The centre panel shows a similar measurement, but for a beat note between a sample of the amplified comb with a stable continuous wave reference laser. In this case, the beat note is stabilized using the repetition rate actuators of the oscillator. This beat frequency can also be well locked, with an integrated phase noise below 0.2 rad. These low phase noises verify that the amplified beam can be used as a frequency comb.

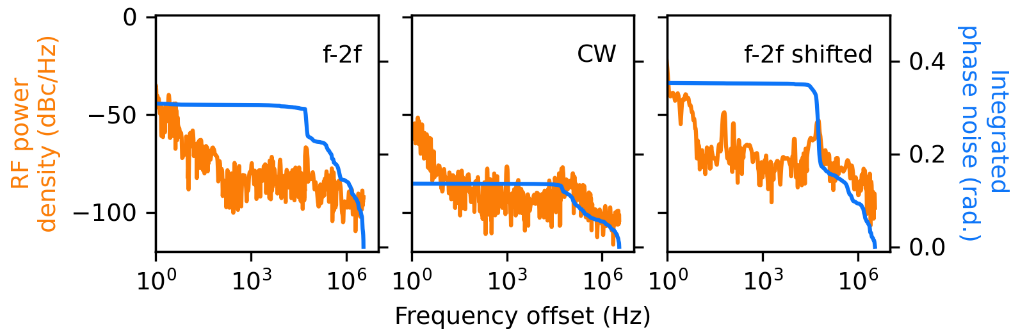

Fig. S6. Measured beat frequencies (orange) of in-loop locking signals of the f-2f signal locked by oscillator CEO actuators, or a CW reference beating with a comb line locked by repetition rate actuators. Conversion of the beat note to integrated phase noise (blue) is also shown, with values well below 1 radian, verifying good lock quality. This shows that the nonlinear amplification does not badly scramble the phase, and that the amplifier can generate high power frequency combs at 100 MHz repetition rate. The right plot uses an optical frequency shifter for a CEO value of -10 kHz.

Conventional f-2f interferometry stabilizes the CEO frequency at a MHz-level value due to the $1/f$ nature of electronic noise. For carrier envelope stable applications, we modified the standard f-2f arrangement as shown in Fig. S7. Spatially splitting the f and 2f beams allows the insertion of an acousto-optic frequency shifter. For zero or small CEO frequencies, the beat note will be near the 230 MHz shifting value, allowing for standard electronic locking at MHz frequencies. We were also able to lock this shifted beat note with similar integrated phase noise, enabling locking of CEO at and near zero frequency. An example for CEO of -10 kHz is plotted in the right of Fig. S6.

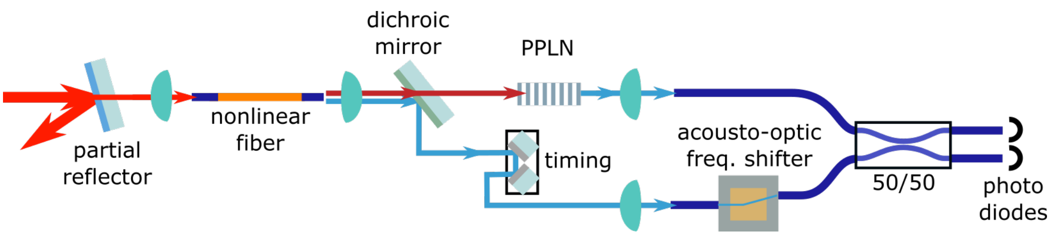

Fig. S7. Schematic of f-2f interferometer with frequency shifter. By shifting the optical frequency of one arm and locking near the shifting frequency, the carrier envelope offset can be locked to small frequencies at and near zero.

REFERENCES

1. M. A. Vorontsov, G. W. Carhart, and J. C. Ricklin, "Adaptive phase-distortion correction based on parallel gradient-descent optimization," Opt. Lett. **22**, 907–909 (1997).
2. F. Köttig, D. Schade, J. R. Koehler, P. S. J. Russell, and F. Tani, "Efficient single-cycle pulse compression of an ytterbium fiber laser at 10 MHz repetition rate," Opt. Express **28**, 9099–9110 (2020).